Journal of Solid State Chemistry 200 (2013) 349–353

Contents lists available at SciVerse ScienceDirect

Journal of Solid State Chemistry

journal homepage: www.elsevier.com/locate/jssc

Synthesis, crystal structure, and optical properties of $Ba_2Cu_2ThS_5$, and electronic structures of $Ba_2Cu_2ThS_5$ and $Ba_2Cu_2US_5$

Adel Mesbah [a], Sébastien Lebègue [b], Jordan M. Klingsporn [a], Wojciech Stojko [a], Richard P. Van Duyne [a], James A. Ibers [a,*]

[a] Department of Chemistry, Northwestern University, 2145 Sheridan Road, Evanston, IL 60208-3113, United States
[b] Laboratoire de Cristallographie, Résonance Magnétique, et Modélisations CRM2 (UMR UHP-CNRS 7036), Faculté des Sciences et Techniques, Université de Lorraine, BP 70239, Boulevard des Aiguillettes, 54506 Vandoeuvre-lès-Nancy Cedex, France

ARTICLE INFO

Article history:
Received 19 November 2012
Received in revised form
8 January 2013
Accepted 13 January 2013
Available online 13 February 2013

Keywords:
Single-crystal X-ray structure
Barium copper actinide sulfides
Optical properties
Electronic structures
Band gaps

ABSTRACT

The compound $Ba_2Cu_2ThS_5$ has been synthesized by the reaction of BaS, S, Cu, and Th at 1173 K. It crystallizes in the monoclinic space group C^3_{2h}–$C2/m$ with two formula units in a cell of dimensions a=13.5616(8) Å, b=4.1159(2) Å, c=9.3548(6) Å, β=115.89(1)° (100 K). The structure comprises Ba^{2+} cations and $^2_\infty[Cu_2ThS_5^{4-}]$ layers. The two dimensional layers are formed by the connection of ThS_6 octahedra and CuS_4 tetrahedra along [001] with a sequence…. *oct tet tet oct tet tet*…. Optical measurements performed on $Ba_2Cu_2ThS_5$ indicate an indirect band gap of 1.86 eV. DFT calculations performed with the HSE06 functional yield band gaps of 1.7 eV for $Ba_2Cu_2ThS_5$ and 1.5 eV for the isostructural compound $Ba_2Cu_2US_5$.

1. Introduction

Interest in actinide chalcogenides stems not only from their varied structures but also from their magnetic, optical, and electrical properties that are associated with the more diffuse 5*f* orbitals versus the 4*f* orbitals of the rare-earth elements. Many alkali-metal ternary and quaternary actinide (poly)chalcogenides have been synthesized [1–12] with the use of the reactive flux method [13]. However, only a few ternary [6,14–22] and even fewer quaternary alkaline-earth actinide chalcogenides have been reported. These include $Ba_4Cr_2US_9$ [23], $Ba_8Hg_3U_3S_{18}$ [24], and $Ba_2Cu_2US_5$ [25]. The latter paper included synthesis, structure, and magnetic properties. In this paper we present the synthesis, structure, and optical properties of $Ba_2Cu_2ThS_5$, the isostructural Th analogue of $Ba_2Cu_2US_5$, and in addition we present the electronic structures of both compounds, as calculated by DFT methods involving the HSE06 functional.

2. Experimental

2.1. Synthesis

The starting reactants, Th powder (MP Biomedicals, LLC 99.1%), Cu (Aldrich, 99.5%), BaS (Alfa, 99.7%), and S (Mallinckrodt, 99.6%), were used as obtained.

$Ba_2Cu_2ThS_5$ was obtained by the combination of Th (20 mg, 0.086 mmol), Cu (10.9 mg, 0.17 mmol), BaS (29.1 mg, 0.17 mmol), and S (13.8 mg, 0.43 mmol). The mixture was loaded into a carbon-coated fused-silica tube under an Ar atmosphere in a glove box. The tube was evacuated to 10^{-4} Torr, flame sealed, and placed in a computer-controlled furnace. The tube was heated to 1173 K, kept at this temperature for 4 d, then cooled to 473 K at 3 K/h, and then the furnace was turned off. Orange needles in about 10 wt% yield based on Th were isolated, and a few were analyzed by EDX to show Ba:Cu:Th:S ≈ 2:2:1:5.

2.2. Structure determination

Single-crystal X-ray data for $Ba_2Cu_2ThS_5$ were collected at 100(2) K by the use of a Bruker APEX II Kappa diffractometer equipped with graphite monochromatized Mo$K\alpha$ (λ=0.71073 Å) radiation. The data collection strategy comprised ω and φ scans obtained from an algorithm in COSMO in APEX II [26]. The step size was 0.3° and the frame time was 10 s/frame. Recorded data were indexed, refined, and integrated by SAINT in the APEX II package [26]. Face-indexed absorption, incident beam, and possible decay corrections were performed with the use of the program SADABS [27]. The structure of $Ba_2Cu_2ThS_5$ was solved and refined with the programs SHELXS and SHELXL [28], respectively. The atomic positions were standardized with the program STRUCTURE TIDY [29] in PLATON [30]. Crystal structure data and refinement details are provided in Table 1 and in Supporting material. Selected interatomic distances are reported in Table 2.

* Corresponding author. Fax: +1 847 491 2976.
E-mail address: ibers@chem.northwestern.edu (J.A. Ibers).

0022-4596/$ - see front matter © 2013 Elsevier Inc. All rights reserved.
http://dx.doi.org/10.1016/j.jssc.2013.01.016

2.3. Optical measurements

Single-crystal optical absorption measurements from 1.4 eV (889 nm) to 3.9 eV (318 nm) were performed at 298 K with a Nikon Eclipse Ti2000-U inverted microscope. A goniometer mounted to the inverted microscope with a custom holder held a single crystal of $Ba_2Cu_2ThS_5$ at the microscope focal point. A tungsten halogen lamp acted as the illumination source for the absorption measurements. Polarized measurements were performed by filtering the light source to select a single polarization. The absorption spectra were collected using a 40× extra-long working distance objective. The light was spatially filtered with a 200 μm aperture to eliminate light not transmitted through the crystal and provided a 5 μm spot at the region of interest. Light was dispersed by a 150 groove/mm grating in an Acton SP2300 imaging spectrometer. The dispersed light was then collected on a back-illuminated LN_2-cooled CCD (Spec10:400BR, Princeton Instruments). All spectra were collected for 70 μs and accumulated 200 times.

2.4. Computational calculations (DFT)

We have performed our calculations using density functional theory [31] based on the Kohn-Sham equation [32]. In particular, we have used the HSE06 exchange-correlation potential [33–35]. This functional has a part of the Hartree-Fock potential for the short-range region of the Coulomb interaction while the correlation is at the generalized gradient level (GGA) [36]. The HSE06 functional solves at least partly the problem of self-interaction to give band gaps that are usually in reasonable agreement with experiments. To perform the calculations, we have used the Vienna ab initio Simulation Package (VASP) [37,38] that implements the projector augmented wave method [39]. For both $Ba_2Cu_2ThS_5$ and $Ba_2Cu_2US_5$ a k-point grid of $6\times6\times4$ was found to be sufficient to enable convergence of the integrations in the Brillouin zone, and the plane-wave cut-off was set to its default value. The experimental geometry (lattice parameters and positions of the atoms) was used without further relaxation, and spin polarization was allowed. The optical properties in the sum-over-states approximation were implemented [40] in the VASP code.

Table 1
Crystallographic data and structure refinements for $Ba_2Cu_2ThS_5$.[a]

Space group	C^3_{2h}–C2/m
a (Å)	13.5616(8)
b (Å)	4.1159(2)
c (Å)	9.3548(6)
β (deg.)	115.891(4)
V (Å^3)	469.76(5)
Z	2
ρ (g cm^{-3})	5.615
μ (mm^{-1})	29.513
R (F)[b]	0.0238
R_w (F_o^2)[c]	0.0477

[a] $\lambda=0.71073$ Å, $T=100(2)$ K.
[b] $R(F)=\sum||F_o|-|F_c||/\sum|F_o|$ for $F_o^2>2\sigma(F_o^2)$.
[c] $R_w(F_o^2)=\{\sum[w(F_o^2-F_c^2)^2]/\sum wF_o^4\}^{1/2}$. For $F_o^2<0$, $w^{-1}=\sigma^2(F_o^2)$; for $F_o^2\geq0$, $w^{-1}=\sigma^2(F_o^2)+(qF_o^2)^2$ where $q=0.0188$.

Table 2
Selected interatomic distances in (Å) of $Ba_2Cu_2ThS_5$.

Atom–Atom	Distance (Å)
Th(1)–S(1)	2.743(1) × 2
Th(1)–S(2)	2.8093(9) × 4
Cu(1)–S(1)	2.3924(7) × 2
Cu(1)–S(2)	2.396(2)
Cu(1)–S(3)	2.3005(7)
Th (1)–Cu(1)	3.2901(6) × 8
Ba(1)–S(1)	3.167(1) × 2
Ba(1)–S(1)	3.398(1)
Ba(1)–S(2)	3.415(1) × 2
Ba(1)–S(2)	3.399(1)
Ba(1)–S(3)	3.0656(3) × 2

3. Results

3.1. Synthesis

Single crystals of the compound $Ba_2Cu_2ThS_5$ were obtained directly at 1173 K , but in a low yield of about 10 wt% based on Th. The analysis of the whole sample showed the presence of powdered $Ba_2Cu_2ThS_5$ and ThOS, the latter being a common contaminant in Th chalcogenide solid-state chemistry [41]. The U analogue, $Ba_2Cu_2US_5$, [25] was obtained earlier in higher yield by a two-step synthesis.

3.2. Structure

$Ba_2Cu_2ThS_5$ crystallizes in the $Ba_2Cu_2US_5$ [25] structure type with two formula units in the monoclinic space group C^3_{2h} – C2/m in a cell of dimensions $a=13.5616(8)$ Å, $b=4.1159(2)$ Å, $c=9.3548(6)$ Å, $\beta=115.89(1)^\circ$ (100 K). In the asymmetric unit there is one Th atom, one Ba atom, one Cu atom, and three S atoms (S1, S2, and S3); their respective site symmetries are 2/m, m, m,m, m, and 2/m.

A general projection of the structure down the b-axis is presented in Fig. 1. Metrical data are given in Table 2. The Th atom is coordinated by six S atoms in a distorted octahedron. The Cu atom is coordinated by four S atoms in a distorted tetrahedron. The Ba atom is coordinated by eight S atoms in a bicapped trigonal prism. The ThS_6 octahedra form infinite chains along [0 1 0] by edge sharing. The CuS_4 tetrahedra form Cu_2S_7 dimers by corner sharing. The structure consists of $^2_\infty[Cu_2ThS_5^{4-}]$ layers separated by Ba atoms. The two-dimensional $^2_\infty[Cu_2ThS_5^{4-}]$ layer (Fig. 2) is built from ThS_6 octahedra and CuS_4 tetrahedra. The connectivity of the MS_n polyhedra within the layer in the [0 0 1] direction is *oct tet tet oct tet tet*. There are no S–S bonds in the structure so charge balance is achieved with formal oxidation states +2, +1, and −2 assigned to Ba, Cu, and S, respectively. The compound can thus be written as $(Ba^{2+})_2(Cu^{1+})_2(Th^{4+})(S^{2-})_5$.

The Th–S distances, which range from 2.743(1) Å to 2.809(1) Å, are comparable to those found in $KCuThS_3$, $K_2Cu_2ThS_4$, and $K_3Cu_3Th_2S_7$ [42]. The Cu–S distances, which range from 2.3005(7) Å to 2.396(2) Å, are comparable to those found in the

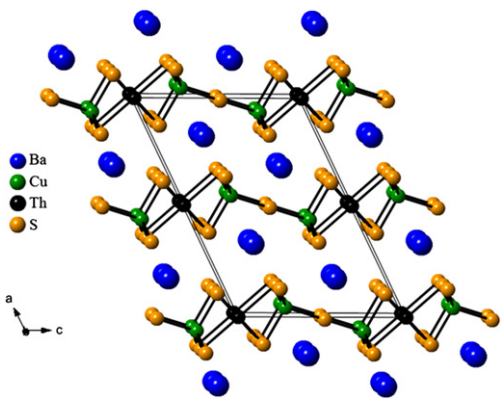

Fig. 1. General view of the structure of $Ba_2Cu_2ThS_5$ along [0 1 0].

$Ba_2Cu_2US_5$ analogue [25] and in $K_2Cu_3US_5$ [12]. The Ba–S distances, which range between 3.0656(3) Å and 3.415(2) Å, are typical of those found in the alkaline-earth actinide chalcogenide ternaries [22].

3.3. Optical results

A fundamental absorption edge (Fig. 3) is observed in the absorption spectrum of $Ba_2Cu_2ThS_5$. A determination of the band gap as either direct or indirect was performed by comparison of the plot of $\alpha h\upsilon$ versus energy ($h\upsilon$) to the plots of $(\alpha h\upsilon)^2$ and $(\alpha h\upsilon)^{1/2}$ versus $h\upsilon$ [43]. These plots show that the semiconducting crystal has an indirect band gap. A value of the optical band gap of 1.86 eV was determined using linear regression analysis of the baseline and absorption edge, as previously described (Fig. 3) [44]. No polarization dependence was observed when polarized transmission spectra were recorded from 0° to 360° in increments of 10°.

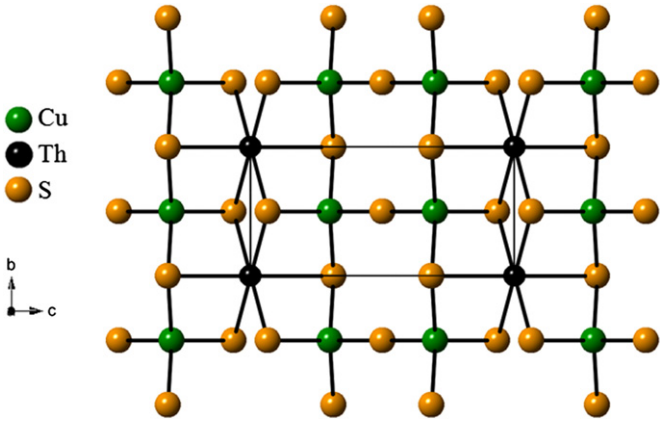

Fig. 2. The structure of the $^2_\infty[Cu_2ThS_5^{4-}]$ layer projected down the *a*-axis.

3.4. Theoretical results

Our computed total and orbital resolved partial density of states (PDOS) are presented from −5 eV to 5 eV in Figs. 4 and 5 for $Ba_2Cu_2ThS_5$ and $Ba_2Cu_2US_5$, respectively. The Fermi level is put at 0 eV. Spin polarization was allowed in our calculations. $Ba_2Cu_2ThS_5$ was found to be non-magnetic. From the total density of states (see upper panel in Fig. 4) $Ba_2Cu_2ThS_5$ has a significant band gap of 1.7 eV that separates the top of the valence bands made up of S1-*p*, S2-*p*, S3-*p*, and Cu-*d* states from the bottom of the conduction bands composed mainly of Th-*d* states. From −5 eV to 0 eV the states originate mainly from Cu-'*d*' states together with the S-*p* states. Notice that the Th-*d* states contribute significantly at −4 eV. The conduction band up to 5 eV is mainly derived from Ba-*d*, Th-*d*, and Th-*f* states. The bonding between the different atoms is difficult to analyze from the PDOS because the S1, S2, S3, and Cu PDOS show considerable structures that cannot be easily related to each other, whereas the Ba PDOS and the Th PDOS display some low values below the Fermi level.

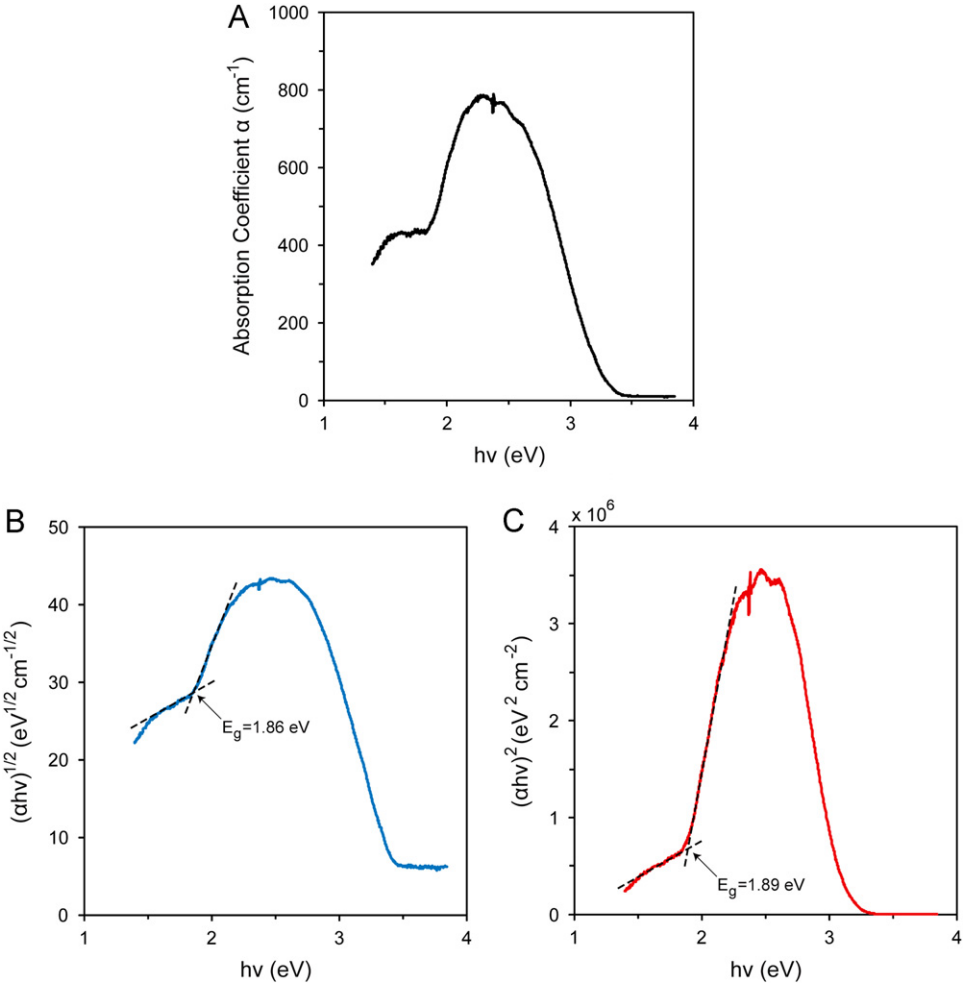

Fig. 3. (A) Absorption spectrum plotted as α vs. $h\upsilon$ (eV); (B) calculated spectrum for an indirect band gap; (C) calculated spectrum for a direct band gap.

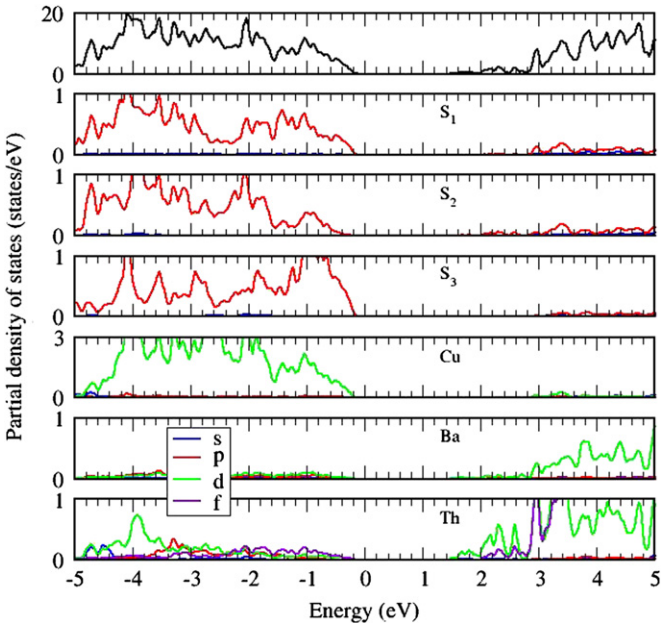

Fig. 4. Total (upper plot) and partial density of states (lower plots) for $Ba_2Cu_2ThS_5$. For each atom, the partial density of state is projected on the relevant orbitals.

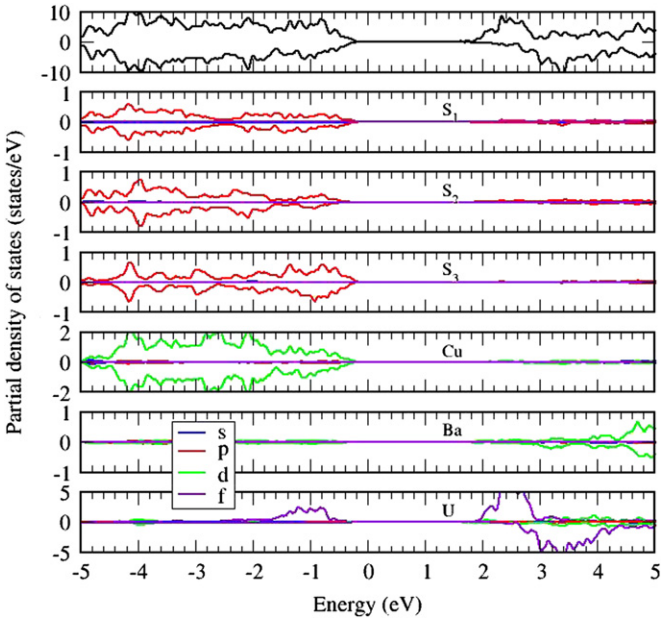

Fig. 5. Total (upper plot) and partial density of states (lower plots) for $Ba_2Cu_2US_5$. For each atom, the partial density of state is projected on the relevant orbitals.

$Ba_2Cu_2US_5$, which contains U^{4+}, was found to be magnetic, in agreement with experiment [25]. Therefore for $Ba_2Cu_2US_5$ spin-polarized PDOS are presented. $Ba_2Cu_2US_5$ also has a significant band gap with a calculated value of 1.5 eV (Fig. 5). All the atoms seem to contribute to the top of the valence bands, whereas the bottom of the conduction bands originates from U-*f* states together with a contribution from the S atoms. As for $Ba_2Cu_2ThS_5$, the states between −5 eV and 0 eV correspond to Cu-*d* and S-*p* states, but for $Ba_2Cu_2US_5$ the *f* shell of the U is now partly filled and therefore contributes as well to the density of states of the valence electrons. For the conduction bands up to 5 eV, all the atoms in $Ba_2Cu_2US_5$ are contributing. Moreover, the magnetic moment of the U atoms is clearly seen from the corresponding PDOS, and it induces a slight spin-polarization on other atoms that can be seen mainly for states just below the Fermi level (from −2 eV to 0 eV).

The imaginary part of the dielectric function for $Ba_2Cu_2ThS_5$ is shown in Fig. 6. Only the diagonal elements of the dielectric tensor are shown, the off-diagonal ones being rather small in magnitude. For the three functions shown in Fig. 6 we observe very similar behaviors, with a small weight from about 1.8 eV to 3 eV but a rapid increase starting from 3 eV. Therefore, apart from the large number of peaks corresponding to the different direct transitions allowed among valence and conduction bands, little anisotropy is observed in the optical properties of $Ba_2Cu_2ThS_5$. To have a deeper understanding of the corresponding electronic structure, we have computed the band structure of $Ba_2Cu_2ThS_5$ along some high-symmetry directions of the Brillouin zone (see Fig. 7). The minimum band gap is indirect between the Γ and Z points with a value of 1.7 eV, whereas the minimum direct band gap occurs at the Z point with a value of 1.8 eV, in good agreement with our calculated dielectric function. In our previous study [21] on Ba_2ThS_6, we found an excellent agreement between the calculated and the experimental values of the band gap. This is confirmed again here for $Ba_2Cu_2ThS_5$. Hence, we believe that the HSE functional [33–35] is a suitable tool to study the electronic structures of materials containing actinides beyond the usual semiconductors and metals [45].

To understand quantitavely the electron distributions in $Ba_2Cu_2ThS_5$ and $Ba_2Cu_2US_5$, we have used Bader's theory of atoms in molecules [46]. To do this for the PAW method (as used here), the reconstructed valence charge density has to be used [47] and not just the bare pseudo-density or else the correctness of the results is uncertain. It appears that the two compounds have very close distributions of valence electrons: all the S atoms have around $7.2e^-$, with a maximum difference of 0.1 between inequivalent S atoms, the Ba atoms have $8.4e^-$, the Cu atoms have $10.6e^-$, and the Th atoms in $Ba_2Cu_2ThS_5$ have $10.0e^-$ and the U atoms in $Ba_2Cu_2US_5$ have $12.0e^-$. Therefore, although the '*f*' shell of the actinide atom becomes partly filled in $Ba_2Cu_2US_5$ and spin-polarized, this has only a minor effect on the electron distribution.

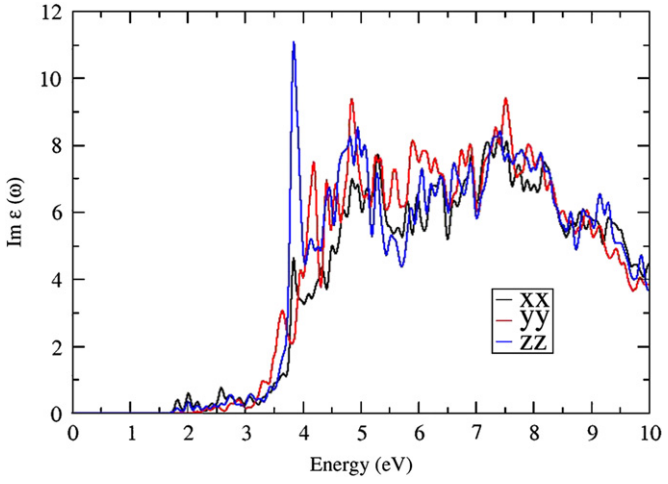

Fig. 6. Calculated imaginary part of the diagonal of the dielectric tensor of $Ba_2Cu_2ThS_5$ for the three independent directions in the crystal.

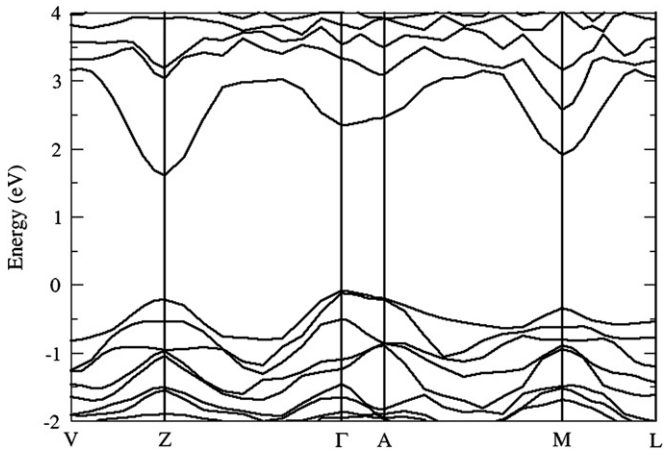

Fig. 7. Calculated band structure along some high-symmetry directions for $Ba_2Cu_2ThS_5$.

4. Conclusions

The compound $Ba_2Cu_2ThS_5$ was synthesized by direct combination of the elements at 1173 K. From single-crystal X-ray diffraction data the compound crystallizes in the monoclinic system in the $Ba_2Cu_2US_5$ structure type. The structure is composed of alternating $^2_\infty[Cu_2ThS_5^{4-}]$ layers and Ba^{2+} cations along the *a*-axis. DFT calculations performed with the HSE06 exchange-correlation potential predict that $Ba_2Cu_2ThS_5$ should be not be magnetic but should be a semiconductor with a band gap of 1.7 eV; optical measurements indicate an indirect band gap of 1.86 eV. The DFT calculations predict that $Ba_2Cu_2US_5$ should be magnetic, in agreement with experiment, with an indirect band gap of 1.5 eV. This agreement between theory and experiment confirms that the HSE06 functional is a suitable tool to study the electronic structures of materials containing actinides beyond the usual semiconductors and metals.

Supporting material

The crystallographic data for $Ba_2Cu_2ThS_5$ have been deposited with FIZ Karlsruhe as CSD numbers 425437, These data may be obtained free of charge by contacting FIZ Karlsruhe at +49 7247808666 (fax) or crysdata@fiz-karlsruhe.de (email).

Acknowledgments

This research was kindly supported at Northwestern University by the U.S. Department of energy, Basic Energy Sciences, Chemical Sciences, Biosciences, and Geosciences Division and Division of Materials Science and Engineering Grant ER-15522. Use was made of the IMSERC X-ray Facility at Northwestern University, supported by the International Institute of Nanotechnology (IIN). Funding for optical studies was provided by the National Science Foundation Grant CHE-1152547 and the NSF MRSEC (DMR-1121262) at the Materials Research Center of Northwestern University.

Appendix A. Supporting information

Supplementary data associated with this article can be found in the online version at: http://dx.doi.org/10.1016/j.jssc.2013.01.016.

References

[1] J.A. Cody, J.A. Ibers, Inorg. Chem. 34 (1995) 3165–3172.
[2] A.C. Sutorik, M.G. Kanatzidis, Chem. Mater. 9 (1997) 387–398.
[3] K.-S. Choi, R. Patschke, S.J.L. Billinge, M.J. Waner, M. Dantus, M.G. Kanatzidis, J. Am. Chem. Soc. 120 (1998) 10706–10714.
[4] B.C. Chan, Z. Hulvey, K.D. Abney, P.K. Dorhout, Inorg. Chem. 43 (2004) 2453–2455.
[5] H. Mizoguchi, D. Gray, F.Q. Huang, J.A. Ibers, Inorg. Chem. 45 (2006) 3307–3311.
[6] A.A. Narducci, J.A. Ibers, Inorg. Chem. 39 (2000) 688–691.
[7] K. Chondroudis, M.G. Kanatzidis, J. Am. Chem. Soc. 119 (1997) 2574–2575.
[8] K.-S. Choi, M.G. Kanatzidis, Chem. Mater. 11 (1999) 2613–2618.
[9] R.H. Hess, P.L. Gordon, C.D. Tait, K.D. Abney, P.K. Dorhout, J. Am. Chem. Soc. 124 (2002) 1327–1333.
[10] K. Chondroudis, M.G. Kanatzidis, C. R. Acad. Sci. Paris 322 (1996) 887–894.
[11] A.C. Sutorik, R. Patschke, J. Schindler, C.R. Kannewurf, M.G. Kanatzidis, Chem. Eur. J. 6 (2000) 1601–1607.
[12] D.L. Gray, L.A. Backus, H.-A.Krug von Nidda, S. Skanthakumar, A. Loidl, L. Soderholm, J.A. Ibers, Inorg. Chem. 46 (2007) 6992–6996.
[13] S.A. Sunshine, D. Kang, J.A. Ibers, J. Am. Chem. Soc. 109 (1987) 6202–6204.
[14] M. Komac, L. Golic, D. Kolar, B.S. Brcic, J. Less-Common Met. 24 (1971) 121–128.
[15] R. Brochu, J. Padiou, D. Grandjean, C. R. Seances Acad. Sci. Ser. C 271 (1970) 642–643.
[16] R. Lelieveld, D.J.W. IJdo, Acta Crystallogr. Sect. B: Struct. Crystallogr. Cryst. Chem. 36 (1980) 2223–2226.
[17] R. Brochu, J. Padiou, J. Prigent, C. R. Seances Acad. Sci. Ser. C 274 (1972) 959–961.
[18] R. Brochu, J. Padiou, J. Prigent, C. R. Acad. Sci. Paris 270 (1970) 809–810.
[19] M. Potel, R. Brochu, J. Padiou, Mater. Res. Bull. 10 (1975) 205–208.
[20] A.A. Narducci, J.A. Ibers, Inorg. Chem. 37 (1998) 3798–3801.
[21] A. Mesbah, E. Ringe, S. Lebègue, R.P. Van Duyne, J.A. Ibers, Inorg. Chem. 51 (2012) 13390–13395.
[22] A. Mesbah, J.A. Ibers, J. Solid State. 199 (2013) 253–257.
[23] J. Yao, J.A. Ibers, Z. Anorg. Allg. Chem. 634 (2008) 1645–1647.
[24] D.E. Bugaris, J.A. Ibers, Inorg. Chem. 51 (2012) 661–666.
[25] H.-yi Zeng, J. Yao, J.A. Ibers, J. Solid State Chem. 181 (2008) 552–555.
[26] Bruker APEX2 Version 2009.5-1 and SAINT version 7.34a Data Collection and Processing Software, Bruker Analytical X-Ray Instruments, Inc., Madison, WI, USA, 2009.
[27] G.M. Sheldrick, SADABS, Department of Structural Chemistry, University of Göttingen, Göttingen, Germany, 2008.
[28] G.M. Sheldrick, Acta Crystallogr. Sect. A: Found. Crystallogr. 64 (2008) 112–122.
[29] L.M. Gelato, E. Parthé, J. Appl. Crystallogr. 20 (1987) 139–143.
[30] A.L. Spek, PLATON, A Multipurpose Crystallographic Tool, Utrecht University, Utrecht, The Netherlands, 2008.
[31] P. Hohenberg, W. Kohn, Phys. Rev. 136 (1964) 864–871.
[32] W. Kohn, L.J. Sham, Phys. Rev. 140 (1965) 1133–1138.
[33] J. Heyd, G.E. Scuseria, M. Ernzerhof, J. Phys. Chem. 118 (2003) 8207–8215.
[34] J. Paier, M. Marsman, K. Hummer, G. Kresse, I.C. Gerber, J.G. Angyan, J. Chem. Phys. 125 (2006) 249901-1-2.
[35] J. Heyd, G.E. Scuseria, M. Ernzerhot, J. Chem. Phys. 124 (2006) 219906-1.
[36] J.P. Perdew, K. Burke, M. Ernzerhof, Phys. Rev. Lett. 77 (1996) 3865–3868.
[37] G. Kresse, J. Forthmüller, Comput. Mater. Sci. 6 (1996) 15–50.
[38] G. Kresse, D. Joubert, Phys. Rev. B 59 (1999) 1758–1775.
[39] P.E. Blöchl, Phys. Rev. B 50 (1994) 17953–17979.
[40] M. Gajdos, K. Hummer, G. Kresse, J. Furthmüller, F. Bechstedt, Phys. Rev. B 73 (2006) 045112-1-9.
[41] L.A. Koscielski, E. Ringe, R.P. Van Duyne, D.E. Ellis, J.A. Ibers, Inorg. Chem. 51 (2012) 8112–8118.
[42] H.D. Selby, B.C. Chan, R.F. Hess, K.D. Abney, P.K. Dorhout, Inorg. Chem. 44 (2005) 6463–6469.
[43] T.-H. Bang, S.-H. Choe, B.-N. Park, M.-S. Jin, W.-T. Kim, Semicond. Sci. Technol. 11 (1996) 1159–1162.
[44] K. Mitchell, F.Q. Huang, A.D. McFarland, C.L. Haynes, R.C. Somers, R.P. Van Duyne, J.A. Ibers, Inorg. Chem. 42 (2003) 4109–4116.
[45] T.M. Henderson, J. Paier, G.E. Scuseria, Phys. Status Solidi B 248 (2011) 767–774.
[46] R.F.W. Bader, Atoms in Molecules: A Quantum Theory, International Series of Monographs on Chemistry, 22, Oxford University Press, Inc., New York, 1990.
[47] E. Aubert, S. Lebègue, M. Marsman, T.T.Thu Bui, C. Jelsch, S. Dahaoui, E. Espinosa, J.G. Angyán, J. Phys. Chem. A115 (2011) 14484–14494.